Available online at www.sciencedirect.com
SCIENCE DIRECT
Journal of Catalysis 240 (2006) 23–30
JOURNAL OF CATALYSIS
www.elsevier.com/locate/jcat

Catalytic oxidation performance of the α-Keggin-type vanadium-substituted heteropolymolybdates: A density functional theory study on $[PV_nMo_{12-n}O_{40}]^{(3+n)-}$ ($n = 0$–3)

Jinyue Wang [a,b], Changwei Hu [a,*], Min Jian [a], Jin Zhang [a], Guiying Li [a]

[a] *Key Laboratory of Green Chemistry and Technology (Sichuan University), Ministry of Education, College of Chemistry, Sichuan University, Chengdu, 610064, China*

[b] *Department of Chemistry and Chemical Engineering, Yibin University, Yibin, 644007, China*

Received 10 December 2005; revised 4 March 2006; accepted 6 March 2006

Available online 3 April 2006

Abstract

O3LYP calculations were carried out to study the structures and properties of the α-Keggin-type vanadium(V)-substituted heteropolyanions $[PV_nMo_{12-n}O_{40}]^{(3+n)-}$ ($n = 0$–3) in an attempt to characterize their catalytic performance. Five α-Keggin $[PV_2Mo_{10}O_{40}]^{5-}$ (**α-PV$_2$**) isomers are studied thoroughly, in comparison with the two β-Keggin isomers of their counterparts and three of the 13 isomers of $[PV_3Mo_9O_{40}]^{6-}$ (**α-PV$_3$**). The d-orbital contribution of vanadium atom to the LUMO (DCVL) of the vanadium-substituted heteropolymolybdates is found to be a key factor in their catalytic performances. Based on this, the activity differences between the five α-PV_2 isomers are predicted and rationalized. A linear correlation between the turnover numbers based on the vanadium atom and the DCVLs is established for the benzene hydroxylation to phenol. The order of the catalytic activities is predicted as $[PMo_{12}O_{40}]^{3-}$ (**α-PV$_0$**) < α-PV_3 < α-PV_2 < $[PVMo_{11}O_{40}]^{4-}$ (**α-PV$_1$**), which is in good agreement with the reported experimental results.

Keywords: Vanadium(V)-substituted heteropolymolybdates; Oxidation catalyst; Redox properties; Benzene hydroxylation; Turnover number; O3LYP

1. Introduction

Polyoxometalates (POMs), especially the heteropoly compounds (HPCs), have attracted much attention in recent years. They not only have been applied as acid catalysts as well as oxidation catalysts in homogeneous and heterogeneous catalytic processes, but also have been used as new materials in the fields of electrochemistry, photochemistry, medicine, and environmental protection [1,2]. The HPCs are attractive because their special structural topology and versatile properties can be tuned at the atomic/molecular levels through modification of the structure type, the central heteroatom, and the transition metal-substituted atoms [3–6].

Among the numerous HPCs that have been synthesized and reported, heteropolymolybdates and tungstates related to the well-known α-Keggin [7] structure have received the most attention and have been systematically studied both experimentally and theoretically. The Keggin core has a special ability to accept electrons without decomposition. In reality, it is a *reservoir* of electrons and thus can undergo many electron-transfer processes without significantly deforming the framework [8]. The general trends for the acid strengths of these Keggin acids are W > Mo (for polyatom) and $P^{5+} > Si^{4+}$ (for the heteroatom) [4]. The oxidation potential (or oxidizing ability) has been reported to be $[PMo_{12}O_{40}]^{3-} > [SiMo_{12}O_{40}]^{4-} \gg [PW_{12}O_{40}]^{3-} > [SiW_{12}O_{40}]^{4-}$ [9]. In addition, the introduction of vanadium(V) into the Keggin framework $[PMo_{12}O_{40}]^{3-}$ is beneficial for redox catalysis [10], shifting its reactivity from acid-dominated to redox-dominated, as demonstrated by the selective oxidation of methanol to either dimethyl ether or formaldehyde [11] and by other selective oxidations of alkanes and aldehydes [12–15]. For polyanions with mixed polyatoms, the oxidation potential is reportedly in the following order: α-PV_2 > α-PV_1 > α-PV_0 [4,9].

* Corresponding author. Fax: +86 28 85411105.
E-mail address: gchem@scu.edu.cn (C. Hu).

0021-9517/$ – see front matter
doi:10.1016/j.jcat.2006.03.005

Notably, the direct selective oxidation of benzene to phenol with hydrogen peroxide as the oxidant is also enhanced by the incorporation of vanadium(V) center into the Keggin heteropolyanion $[PMo_{12}O_{40}]^{3-}$ [16–20]. The activities of the $[PV_nMo_{12-n}O_{40}]^{(3+n)-}$ (n = 1–3) catalysts in the hydroxylation of benzene to phenol in acetonitrile or glacial acetic acid were found to decrease in the following order: α-PV_1 > α-PV_2 > α-PV_3. Electrochemical methods have been used to characterize the reduction potentials of the title compounds [21], revealing that the reduction potentials of these species do not vary monotonically with the number of vanadium atoms substituted. The mono-vanadium-substituted species α-PV_1 exhibits the maximum reduction potential among the polymolybdates, $H_{n+3}PV_nMo_{12-n}O_{40}$ (n = 0–3), and, consequently, it has the greatest oxidation activity; α-PV_2 has a slightly greater reduction potential than α-PV_3. Thus, the order of the reduction potentials for these substituted species is α-PV_1 > α-PV_2 > α-PV_3.

It is well known that positional isomers [22] are always possible and usually coexist in one system when two or more vanadium atoms ($n \geqslant 2$) are incorporated into the α-Keggin framework. There are 5 and 13 positional isomers and enantiomorphs for the α-PV_2 and α-PV_3 species, respectively [22]. These isomers have been identified and characterized by means of ^{31}P and ^{51}V NMR spectrometry [23,24]. In the oxidation of alkanes catalyzed by the $H_5PV_2Mo_{10}O_{40}$ polyoxometalate [25], ^{31}P NMR and ESR measurements are also used to investigate the reactivities of the five inseparable isomers. Studies on the interaction of these α-PV_2 isomers with aldehydes indicate that different isomers show different reactivity [25].

The catalytic performances and reduction potentials obtained for α-PV_2 and α-PV_3 species are the overall effects of all isomers, and the contribution of each isomer cannot be obtained separately from experiments. Thus, revealing the relationship between the structures of these vanadium(V)-substituted heteropolyanions $[PV_nMo_{12-n}O_{40}]^{(3+n)-}$ (n = 0–3) and their catalytic performances both experimentally and theoretically remains an interesting issue.

Although POM/HPC chemistry is an extremely rich area of experimental research, high-level calculations on them are relatively scarce, due mainly to the intensive computational demands imposed by the large size of these species. Weber [26] reported the effect of vanadium substitution on $H_{n+3}PV_nM_{12-n}O_{40}$ (M = Mo, W; n = 0–3) through the X_α calculations and obtained some useful information about their reduction abilities. Most recently, advances in the hardware of computers have made it possible to perform some high-level quantum calculations on these larger systems. Most of the first-principle studies related to the Keggin-type heteropolyanions have been carried out at the Hartree–Fock (HF) and density functional (DF) levels of theory [27–31].

Most recently, Handy and Cohen [32,33] developed an optimized exchange functional OPTX and used it in conjunction with the well-known correlation functional LYP [34] to form two new functionals, the pure functional OLYP and the hybrid functional O3LYP. The latter is defined as in Eq. (1), and the popular B3LYP [34,35] incorporated in Gaussian packages is formulated as Eq. (2) [32,33,36]:

$$\mathrm{O3LYP} = 0.1161*\mathrm{XHF} + 0.9262*\mathrm{XS} + 0.8133*\mathrm{OPTX} + 0.19*\mathrm{VWN5} + 0.81*\mathrm{LYP}, \quad (1)$$

$$\mathrm{B3LYP} = 0.2*\mathrm{XHF} + 0.8*\mathrm{XS} + 0.72*\mathrm{XB88} + 0.19*\mathrm{VWN} + 0.81*\mathrm{LYP}. \quad (2)$$

Here XHF denotes Hartree–Rock exchange; XS denotes Dirac–Slater exchange [37]; XB88 denotes Becke's 1988 nonlocal exchange [38]; VWN denotes Vosko, Wilks, and Nusair's local correlation [39]; and LYP denotes Lee, Yang, and Parr's nonlocal correlation [34]. Besides the different mixing coefficients of the exchange functionals from B3LYP, O3LYP uses the optimized OPTX to substitute the B88 exchange. It is worth noting that the VWN correlation functional in O3LYP is modified to the preferred one, VWN5, which differs from the VWN originally used in B3LYP because they were established based on different models [39].

Compared with the BLYP and B3LYP, the performances of these new functionals have been tested on geometries, energies, heats of reaction, and barrier heights for some molecules and organic reactions [36,40–46]. Results have indicated that both OLYP and O3LYP are among the best functionals currently available, and the OLYP is a great improvement over BLYP on both energy and structure parameters for certain systems. It was also found that although in some cases, especially in dealing with hydrogen-bonding systems [41], O3LYP underestimated hydrogen bond strengths even more than B3LYP, the O3LYP functional was overall superior to B3LYP, at least in the same quality [36,43,45,46].

Consequently, the aim of the present work is to assess the new hybrid functional O3LYP method on the structures and properties of these transition metal heteropolyanion clusters. The focus is on the substitution effects of the vanadium(V)-substituted heteropolymolybdates $[PV_nMo_{12-n}O_{40}]^{(3+n)-}$ (n = 0–3) in an attempt to characterize theoretically the relationship between the structures and their catalytic oxidation abilities, especially the varying behaviors among the five α-PV_2 isomers.

2. Models and computational approach

The α-Keggin anion $[PMo_{12}O_{40}]^{3-}$ as shown in Fig. 1 comprises an assembly of 12 corner-shared octahedra MoO_6 from trimetallic groups $\{Mo_3O_{13}\}$ around a heteroatom tetrahedron PO_4. Each $\{Mo_3O_{13}\}$ group exhibits an edge-sharing octahedral. The corner-shared oxygen atoms connecting the trimetallic group are denoted as O_c, and the edge-shared ones in each trimetallic group are denoted as O_e. The internal oxygen atoms between the central tetrahedron and the trimetallic groups are noted as O_i. The terminal oxygen atom, bounded to only one molybdenum atom, is denoted as O_t. The corresponding molecular structure of the α-Keggin heteropolyanion $[PMo_{12}O_{40}]^{3-}$ is shown in Fig. 2a.

In the present work, following Pope [22] and Pettersson [23], we also indicate the vanadium positions in the α-PV_2 species by the lowest possible numbers (1, x for the α-isomers, as shown

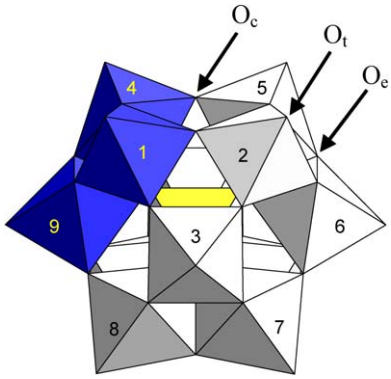

Fig. 1. Polyhedral representation of α-Keggin $[PMo_{12}O_{40}]^{3-}$. The central light grey (yellow in web version) part is the PO_4 tetrahedron, the darkly grey (blue in web version) part is one of the trimetallic $\{Mo_3O_{13}\}$ groups.

previously [23]). Thus, the 1,4-, 1,2-, 1,5-, 1,6-, and 1,11-isomers shown in Fig. 1 are denoted as **α-PV_2-A**, **α-PV_2-B**, **α-PV_2-C**, **α-PV_2-D**, and **α-PV_2-E**, respectively. The frequently investigated 1,4,9-isomer (**α-PV_3-A**) and 1,2,3-isomer (**α-PV_3-B**) are chosen to represent the α-PV_3 species. The three vanadium atoms in α-PV_3-A locate in the same trimetallic group $\{V_3O_{13}\}$ and are edge-sharing linked, whereas those in α-PV_3-B are corner-sharing linked, with each located in a separated trimetallic group $\{Mo_2VO_{13}\}$. Besides these two α-PV_3 isomers, another one, 1,5,11 (**α-PV_3-C**), in which the positional character of V atoms is similar to that in the α-PV_2-C and α-PV_2-E isomers, was also studied. Because two β-Keggin di-vanadium-substituted species β-PV_2 detected by Pettersson [22] coexist with the α-Keggin species, they may derive from the preparation or isomerization of the α-Keggin species; we also take them into account to compare them with their counterparts. These two β-Keggin species, 4,10- and 4,11-isomer, are denoted as **β-PV_2-A** and **β-PV_2-B**, respectively. The molecular structure of the β-Keggin anion $[PMo_{12}O_{40}]^{3-}$ is depicted in Fig. 2b.

It is clear that many properties of the HPCs in solution depend on the concentration, the pH value of the solution, the reaction temperature, and other factors. At present, it is impossible to take all of these possible factors into account in a quantum chemical study. In this work, the PCM model [47] was applied to model the effect of the solvent on these polyanions. Calculations were carried out using the Gaussian 03W program packages [48]. All geometries were fully optimized. For such large clusters, the LanL2MB or the LanL2DZ basis sets with quasi-relativistic effective core potentials (ECPs) [49] were chosen to represent the cores and the valence orbitals. The basis set was augmented with a single set of diffuse p-functions and a set of d-polarization function on the central P atom [50]. The energies of all of the clusters investigated were corrected by the zero-point vibrational energy (ZPVE) calculated in the gas phase. The single-point calculations on these anions in solvent were based on the structures optimized in the gas phase, and the energies also contained the ZPVE corrections.

3. Results and discussion

3.1. Verification of the selected method

Bridgeman [31], in a density functional theory study on the vibrational frequencies of α-Keggin heteropolyanions, pointed out that the results from the B3LYP calculations were in close agreement with experimental results, although these calculations were extremely computationally demanding and cannot be considered a standard task for the study of those large, heavy-element cluster anions. Because of this, the initial study aimed to assess the efficiencies of the newly developed hybrid functional O3LYP on the large α-Keggin polyanion $[PMo_{12}O_{40}]^{3-}$ and compare them with those of the popular B3LYP calculations. The α-Keggin structures have T_d symmetry, and thus the optimization was performed under this symmetry constraint. The calculated results and the experimental values are listed in Table 1.

Not surprisingly, the data obtained from our calculations are similar to the data reported by Bridgeman [31] when we used the same B3LYP/LanL2DZ level of theory on the clus-

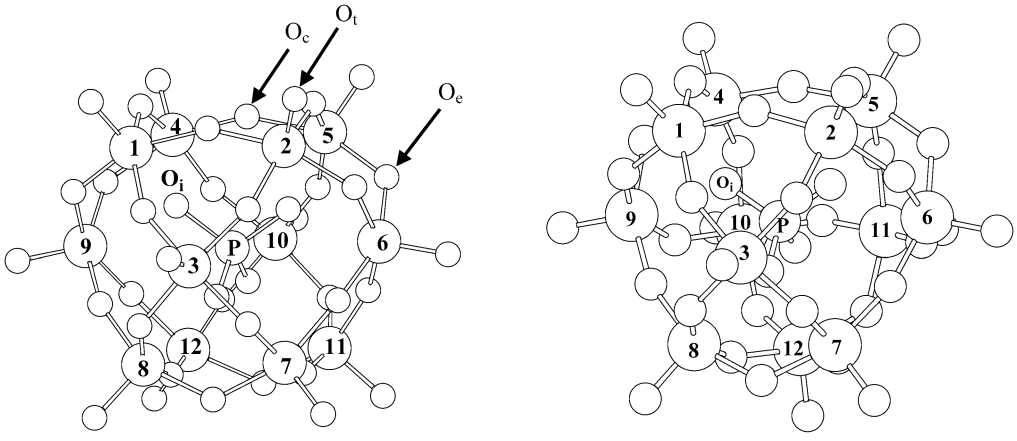

Fig. 2. Perspective plot of the atomic coordination of polyanion $[PMo_{12}O_{40}]^{3-}$. (a) α-Keggin; (b) β-Keggin. The molybdenum atoms are labeled in Arabic numbers. The β-Keggin is generated from α-Keggin by rotating 60° of the trimetallic group $\{Mo_3O_{13}\}$ labeled 10, 11, 12 along its three-fold axis.

Table 1
Computed and experimental parameters of the α-PV_0

Method	Bond length (Å)					Bond angle (degree)		Av% dev[a]	GHL (eV)[b]
	X–O_i	M–O_i	Mo–O_e	Mo–O_c	Mo–O_t	Mo–O_e–Mo	Mo–O_c–Mo		
O3LYP/LanL2MB	1.564	2.465	1.929	1.919	1.722	129.7	149.8	1.53	2.14
O3LYP/LanL2DZ	1.578	2.483	1.946	1.936	1.723	128.5	152.4	1.89	2.80
B3LYP/LanL2MB	1.564	2.465	1.927	1.917	1.723	129.8	150.4	1.49	2.84
B3LYP/LanL2DZ	1.578	2.484	1.944	1.936	1.725	128.6	152.8	1.95	3.29
Exptl.[c]	1.54	2.44	1.91	1.92	1.68	125	151		
Calcd.[d]	1.578	2.484	1.944	1.936	1.725				
Calcd.[e]									2.03

[a] Average deviation between the calculated parameters in this work and the experimental results.
[b] Energy gap between the highest occupied molecular orbital and the lowest unoccupied orbital.
[c] Experimental values from Ref. [51].
[d] Calculated results from Ref. [31].
[e] Calculated result from Ref. [27].

ter (see entries four and six in Table 1). However, if we chose the LanL2MB basis sets, then the structural parameters obtained are also satisfactory (entry three in Table 1). The average percentage deviations (Av% dev) between the calculated parameters in this work and the experimental work (Exptl.) are 1.95 and 1.49, respectively. The same trend was also found for the new functional O3LYP, and the geometry predicted using LanL2MB basis sets is closer to the experimental results than that obtained using LanL2DZ. The average percentage deviations (Av% dev) with the basis sets LanL2DZ and LanL2MB are 1.89 and 1.53, respectively. Comparing the geometrical parameters produced from the B3LYP and O3LYP calculations, the Av% devs are quite close when the same basis sets were used. However, in these cases, the calculated bond lengths are systematically longer than the experimental values, presumably due to the lack of a stabilizing crystal field for the anion when treated as gas-phase species.

One of the important factors affecting the oxidation capacity of these fully oxidized polyanions—the energy gap between the highest occupied molecular orbital (HOMO) and the lowest unoccupied orbital (LUMO) (abbreviated as GHL)—was compared to test these methods (see Table 1). The GHL values calculated using LanL2DZ basis sets are all nearly 0.7 eV larger than those calculated using LanL2MB basis sets with both B3LYP and O3LYP. Even though the calculated GHLs for this polyanion α-PV_0 using Gaussian software packages in this study are larger than the reported value of 2.03 eV (entry seven) using the ADF software with the larger triple-ζ (TZ) basis sets [27], the GHL value computed at O3LYP/LanL2MB level of theory is much closer to the literature data than that calculated at the other three levels, as shown in Table 1.

In addition, we also calculated the vibrational frequencies of the α-PV_0 at the O3LYP/LanL2MB level of theory. The characteristic frequencies of this typical α-Keggin structure are 1069, 1053, 871, and 808 cm^{-1} for the asymmetric stretching of Mo–O_t, P–O_i, Mo–O_c–Mo, and Mo–O_e–Mo, respectively. With the exception of the slightly larger Mo–O_t asymmetric stretching frequency, which in this case is the result of coupling motion with the asymmetric stretch of the P–O_i bond [31], the vibrational frequencies are consistent within a 10 cm^{-1} deviation with the experimental infrared data [52]. Those frequencies predicted at the B3LYP/LanL2MB level are almost the same as those calculated with the O3LYP method.

Table 2
Symmetry used in optimizations, relative energy (E_r), GHL and the solvent effects of the selected species studied. The energies of the α-PV_0, α-PV_2-A, and α-PV_3-A isomers are selected as references for the same charged species, respectively. The data in parentheses are the relative single point energies in the acetonitrile solvent

Species	Symmetry	E_r (kJ mol^{-1})	GHL (eV)	Solvent effect (kJ mol^{-1})
α-PV_0	T_d	0.0 (0.0)	2.14	−905.4
β-PV_0	C_{3v}	55.5 (56.0)	1.94	−904.6
α-PV_1	C_s	–	2.10	−1660.3
α-PV_2-A	C_s	0.0 (0.0)	2.09	−2645.5
α-PV_2-B	C_s	−1.6 (−1.1)	2.08	−2645.1
α-PV_2-C	C_2	−8.4 (−7.3)	2.10	−2644.7
α-PV_2-D	C_1	−5.7 (−4.5)	2.13	−2644.3
α-PV_2-E	C_{2v}	−3.1 (−3.1)	2.03	−2645.5
β-PV_2-A	C_1	52.6 (54.7)	1.98	−2643.4
β-PV_2-B	C_1	45.6 (47.9)	2.00	−2643.4
α-PV_3-A	C_{3v}	0.0 (0.0)	2.11	−3859.0
α-PV_3-B	C_{3v}	−3.4 (−2.5)	2.15	−3858.1
α-PV_3-C	C_s	−18.9 (−17.7)	2.04	−3857.7

In all, calculations at O3LYP/LanL2MB level of theory are quite satisfactory for studying such computationally demanding heteropolyanion compounds. Subsequently, the geometries of the selected $[PV_nMo_{12-n}O_{40}]^{(3+n)-}$ ($n = 0$–3) were fully calculated under the above level of theory O3LYP/LanL2MB. The data are summarized in Table 2.

3.2. Stability of $[PV_nMo_{12-n}O_{40}]^{(3+n)-}$ ($n = 0$–3)

The most frequently studied Keggin type α- and β-isomers have quite different energy levels. As shown in Table 2, the energy level of the β-Keggin anion $[PMo_{12}O_{40}]^{3-}$ is 55.5 kJ/mol higher than that of its α-isomer. In addition, the β-PV_2-A and β-PV_2-B isomers have 52.6 and 45.6 kJ/mol more energy, respectively, than the corresponding α-PV_2-A isomer. The GHL values of all β-Keggin species are slightly lower than those of their α-counterparts. These obvious differences in energies and GHL values indicate that the α-Keggin species are more stable than their β counterparts. Compared with the β-Keggin frame-

works, the favorable stabilities of the α-Keggin clusters may be due to the less obtuse corner-sharing Mo–O–Mo bonds to the rotated $\{V_3O_{13}\}$ group.

For the five α-PV_2 isomers, the energy differences are quite small considering the accuracy of our calculations. Comparing the stability of these isomers is difficult. For example, the energy of the α-PV_2-C is calculated to be the lowest, but it is only 8.4 kJ/mol lower than that of the α-PV_2-A isomer (the highest). This may be the main reason why one isomer is quite difficult to separate from the others experimentally. The discrepancy between the statistically predicted relative abundance and the experimentally observed relative abundance [23,24] may result from their relative stabilities, even though the energy difference obtained in the present work is quite small. For α-PV_2-A and α-PV_2-B, the statistically predicted abundance is 18.2% for both, but the experimentally observed values are 13.3 and 23.3%, respectively.

As more vanadium atoms are incorporated into the Keggin framework, the energy differences become more obvious. As shown in Table 2, the largest energy difference between the five α-PV_2 isomers is 8.4 kJ/mol, whereas that for the three α-PV_3 clusters is as large as 18.9 kJ/mol.

3.3. The solvent effect of acetonitrile

It should be noted that all of the HOMOs and LUMOs of the polyoxoanions have very high energy levels (3.0–9.0 and 6.0–12.0 eV, respectively) because of their large negative charges. It is well known that these highly charged heteropolyanions do not exist in the gas phase and that the external field generated by the solvent and the counterions is crucial to stabilize them. The calculated results of the effect of acetonitrile solvent on these polyoxoanions are given in the last column of Table 2.

After PCM calculations, a considerable decrease in molecular orbital energy and a decrease in the magnitude of the solvent effects occurs in parallel to the charge of these anions. The energies of the HOMOs shift to the negative region, which is a necessary condition for stability. Keep in mind that the heteropolyanions are easily reducible chemical species, and thus the energy of the LUMO must be sufficiently low to accept the incoming electron in catalytic reactions. The solvent molecules in dilute solutions stabilize these anions and place these molecular orbitals at the appropriate level. The energies of the HOMOs and the LUMOs lie in the regions of -6.0 to -3.0 eV and -3.0 to -1.0 eV, respectively. Yet the GHL values of these anions in solution do not vary and are almost the same as those in the gas phase, demonstrating that the intrinsic properties are determined by the molecular structures.

As shown in Table 2, the solvent effects change in parallel to the overall charges of the anions; that is, the greater the negative charge of the anion, the greater the solvent effect. For these charged clusters, the solvent effects are dominated by the electrostatic component–the interactions of the polarized polyanions with the charge distribution of the solvent. In conjunction with the energy changes of the HOMOs and LUMOs of these clusters, when not taking any counter ions or external force fields into account, the electrostatic effects on the properties of the POMs cannot be neglected.

3.4. Redox capacity of $[PV_nMo_{12-n}O_{40}]^{(3+n)-}$ ($n = 0$–3)

It is generally accepted that in the absence of paramagnetic ions, the ground state configuration of heteropolyanions is typical of a fully oxidized polyoxoanion with a high GHL value. Whereas the HOMO primarily delocalizes over the nonbonding p-orbitals of the oxygen atoms, the LUMO usually consists of an antibonding combination of d-orbitals on the molybdenum centers and p-orbitals on the neighboring bridging oxygen atoms O_e and O_c. Moreover, the metal substitution may modify the energy and composition of the LUMO and thus also the redox properties of the cluster. Studies have shown that the substitution of Mo^{6+} ion in Keggin structures by higher electronegativity of V^{5+} ion often increases the oxidation abilities of the POMs [10–15], but does not affect the energies of the HOMOs, which are centered almost entirely on the oxygen [26–28]. Because of this, the HOMOs for these differently charged species are usually treated as oxo-bands [26–29]. Moreover, usually the extra reduction electron preferentially goes to the vanadium atom, leading to the formation of the reduced species with one electron localized on the V center, not the heteropoly-blue with the one electron delocalized among all of the metal centers of the Keggin framework [27].

Therefore, for the differently charged cluster anions $[PV_nMo_{12-n}O_{40}]^{(3+n)-}$ ($n = 0$–3), the energy and composition of the LUMOs have significant effects on the redox properties of the POM [53]. In general, the lower the LUMO energy (i.e., the smaller the GHL value) and the greater the contribution of the vanadium in the LUMO, the easier the species traps additional electrons and thus the more active the cluster in the oxidation reaction. The GHL values of all of the calculated clusters are given in Table 2.

Taking the GHL values of all clusters into account, the data in Table 2 indicate that the GHL values of the β-Keggin species β-PV_0 and β-PV_2 are nearly 0.2 eV lower than those of their corresponding isomer anions α-PV_0 and α-PV_2. Taking their higher electron energies (mentioned earlier) into account, the β-Keggin species are clearly more readily oxidized and less stable than their α-isomers. For the five α-PV_2 isomers, the differences in GHL values are quite small, changing within 0.1 eV. However, the GHL value of the α-PV_2-E isomer is only 2.03 eV, nearly 0.1 eV smaller than the GHL values of the other four isomers.

In the event of similar GHL values for the substituted polyanions, the compositions of the LUMOs are crucial to the investigation into the oxidative properties of these polyanions. Consequently, the LUMO compositions of the α-Keggin heteropolyanions were checked further; the data are summarized in Table 3. As can be seen, the LUMOs consist of the d-orbitals of the Mo and/or V atoms and the p-orbital of the oxygen atom. However, the d-orbital contribution of vanadium atoms to the LUMO (DCVL) does not parallel the mass content of the vanadium-substituted anions. For the α-PV_1 species, the DCVL is 10.5%; with an increasing number of substituted V atoms, the

Table 3
LUMO compositions, DCVLs and the abundance (Abd.) [23,24] of the α-Keggin anions

Species	Composition of LUMO (%)			DCVL	Abd. (%)
	Mo 4d	V 3d	O 2p		
α-PV_0	58.2	–	33.9	–	–
α-PV_1	49.7	10.5	31.5	10.5	100
α-PV_2-A	44.1	16.7	30.0	8.4	18.2
α-PV_2-B	43.7	17.4	29.6	8.7	18.2
α-PV_2-C	40.4	21.8	28.9	10.9	18.2
α-PV_2-D	45.3	14.4	30.7	7.2	36.4
α-PV_2-E	40.4	21.5	29.2	10.7	9.1
α-PV_3-A	44.3	14.0	29.9	4.7	1.82
α-PV_3-B	44.2	14.3	29.6	4.8	1.82
α-PV_3-C	31.2	32.3	24.9	10.8	5.46

DCVL decreases (to nearly 8% for α-PV_2 and 5% for α-PV_3) for all species except α-PV_2-C and α-PV_2-E (10.9 and 10.7%, respectively) and α-PV_3-C (10.8%).

Different positionally substituted V atoms in the Keggin structure may form different chemical environments of vanadium; therefore, the five isomers of the α-PV_2 species may exhibit different oxidation properties. The α-PV_2-D isomer has the largest GHL value, yet the smallest DCVL, among the α-PV_2 species. Whereas the GHL values of α-PV_2-A and α-PV_2-B are quite similar to that of α-PV_2-C, the DCVLs for these first two isomers, in which the two vanadium atoms are neighbor-linked, are smaller than the DCVL of the cluster α-PV_2-C. Considering the experimental fact that α-PV_1 is more active than α-PV_2, the most catalytically active clusters among the α-PV_2 species could be attributed to the α-PV_2-C and α-PV_2-E isomers, not only because their DCVLs are very close to those of the mono-vanadium species, but also because of their special vanadium position in the framework of the Keggin structure. The two vanadium atoms are far located in these two frameworks (5.10 and 7.09 Å in α-PV_2-C and α-PV_2-E, respectively, and 3.32 and 3.52 Å in α-PV_2-A and α-PV_2-B, respectively), making the chemical environment of vanadium very similar to that of the α-PV_1 species.

To confirm this supposition, we propose that the tri-vanadium-substituted configuration, which has both the α-PV_2-C and α-PV_2-E di-vanadium-substituted characteristics, has a different LUMO composition among the 13 isomers of α-PV_3. This supposed configuration is α-PV_3-C (1,5,11-isomer, or its 1,5,8-enatiomorph), in which every two vanadium atoms are separated far apart from each other. This is why we took this isomer into account earlier in the present work. As mentioned above, the calculated result (Table 3) on this cluster shows that its DCVL is 10.8%, quite close to the 10.9% of α-PV_2-C, the 10.7% of α-PV_2-E, and the 10.5% of the mono species α-PV_1. In addition, the GHL value of this isomer is calculated to be 2.04 eV (Table 2), almost the same as 2.03 eV, the lowest value among the five isomers of the α-PV_2 species. Based on these two findings, α-PV_3-C appears to be the most active isomer among the α-PV_3 species.

Nevertheless, from a synthesizing standpoint, we cannot control the reaction conditions to allow these favorable positional vanadium-substituted isomers to be synthesized separately. Moreover, it is well worth pointing out that the statistically relative abundance of these reactive species is not very high in their isomer systems, 18.2% for α-PV_2-C, 9.1% for α-PV_2-E [23], and 5.46% for α-PV_3-C [24]. Altogether, the most reactive clusters for α-PV_2 occupy only 27.3%, which is not compatible with the 100% for α-PV_1 species. This is probably why α-PV_1 exhibits higher catalytic activity.

Therefore, because vanadium is essential to the catalytic properties, and the energy and composition of the LUMO are vital in governing the oxidation activities, the abundance of different isomers may play an important role in catalytic performance. Assuming that the isomers with proper structures of vanadium atoms are active and that others exhibit little activity for benzene hydroxylation, the vanadium atoms incorporated into the α-PV_2-C, α-PV_2-E, and α-PV_3-C isomers may be treated as *active vanadium* in α-PV_2 and α-PV_3, whereas others make little contribution. Due simply to the low ratio of these active vanadium atoms, the oxidation activity of α-PV_2 and α-PV_3 lag behind that of α-PV_1. In none of the isomers of α-PV_2 and α-PV_3 except α-PV_2-C, α-PV_2-E, and α-PV_3-C do the vanadium atoms exhibit activity in benzene hydroxylation and possible activity in other catalytic reactions as well [54].

3.5. Correlation of the predicted oxidation capacity of $[PV_nMo_{12-n}O_{40}]^{(3+n)-}$ ($n = 1$–3) with the TON in benzene hydroxylation [18]

As stated above, the most active clusters of α-PV_2 and α-PV_3 are the isomers α-PV_2-C, α-PV_2-E, and α-PV_3-C. We investigated the relationship of these most active clusters with their catalytic performances in benzene hydroxylation to phenol as performed in acetic acid in our laboratory. In doing so, we checked the DCVLs of the most active vanadium-substituted clusters along with their abundance versus the TONs obtained in the benzene hydroxylation [18], which are plotted in Fig. 3 (line ▲). It is interesting to note that when the relative abundance of the α-PV_2 and α-PV_3 isomers is taken into account [23,24], the nearly linear relationship of the DCVLs of these clusters with per-vanadium TONs is revealed. This result is in line with the reduction potentials derived with electrochemical methods [21]. We questioned whether this linear correlation was just coincident with the benzene hydroxylation performed in acetic acid with hydrogen peroxide in our laboratory.

To verify this correlation of this theoretical work with experiments, we used the available per-vanadium TONs of the hydroxylation of benzene to phenol in acetonitrile solvent [17, 20] to correlate with these DCVLs, which are also plotted in Fig. 3 (lines ○, △, and ▼). It is no accident that we found similar linear correlations between the DCVLs of the most active clusters α-PV_2-C, α-PV_2-E and α-PV_3-C with the catalytic oxidation performance of α-PV_2 and α-PV_3. This linear correlation may somehow reflect the vanadium-substituted effects on the catalytic activity of the heteropolymolybdates applied as catalysts in benzene hydroxylation [55] and other reactions catalyzed by the title compounds [56].

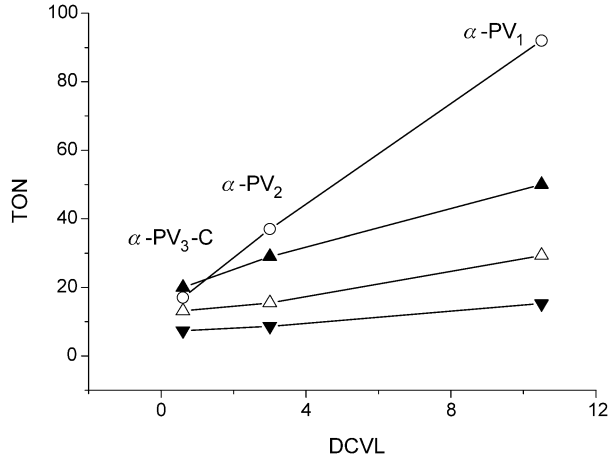

Fig. 3. Correlation of the DCVLs with TONs to phenol in benzene hydroxylation. (○, ▲) data from [17,18], respectively, and (△, ▼) tetrabutylammonium salts and their free acid forms of catalysts in [20], respectively. $DCVL(\alpha\text{-}PV_2) = (DCVL * Abd.)_{\alpha\text{-}PV_2\text{-}C} + (DCVL * Abd.)_{\alpha\text{-}PV_2\text{-}E}$.

As shown in Fig. 3, the lines have different slopes. These differences may be due to the effects of the reaction conditions, like solvent, temperature, counterions, and so on. These differences can be most clearly seen in the two lines (△ and ▼) for the same reaction with different salts of these heteropolymolybdates.

4. Conclusion

The newly developed hybrid density functional O3LYP has proven quite efficient in the computational studies concerning transitional metal clusters like the Keggin POMs. Different positional Mo atom(s) substituted by the V atom(s) in the Keggin structure $[PMo_{12}O_{40}]^{3-}$ may create different vanadium chemical environments, thus causing the title compounds to exhibit varying catalytic performance. For the first time, a nearly linear correlation of the TONs for the catalytic hydroxylation of benzene with the DCVL based on the per-vanadium atom was found. This correlation may be the direct result of vanadium substitution effects on the catalytic hydroxylation capacities for the vanadium-substituted heteropolymolybdates investigated in the present work.

Different isomers, especially for the α-PV_2 species, may exhibit different catalytic activities for different oxidation reactions. The isomers with vanadium in distal positions, especially α-PV_2-C and α-PV_2-E, are the most active clusters for benzene hydroxylation. Therefore, favorable conditions should be created in experiments to prepare the selectively site-substituted vanadium(s) isomers and apply them in the catalytic oxidation of aromatic compounds as well as in catalyzed alkane oxidations.

Acknowledgments

Financial support from the NNSFC (20502017, 20072024) and the Teaching and Research Award Program for Outstanding Young Teachers in Higher Education Institutions is gratefully acknowledged. The authors are also grateful for financial support from the Major Projects of Natural Science, supported by the Bureau of Education of Sichuan Province (2004A182).

Supporting information

The online version of this article contains additional supplementary information.

Please visit DOI:10.1016/j.jcat.2006.03.005.

References

[1] C.L. Hill (Ed.), Chem. Rev. 98 (1998) 1–388 (special issue on the polyoxometalates).
[2] C.L. Hill (Ed.), J. Mol. Catal. A 114 (1996) 1–371 (special issue on the polyoxometalates in catalysis).
[3] T. Okuhara, N. Mizuno, M. Misono, Adv. Catal. 41 (1996) 113.
[4] M. Misono, Catal. Rev.-Sci. Eng. 29 (1987) 269.
[5] J.B. Moffat, Appl. Catal. A 146 (1996) 65.
[6] C.L. Hill, Activation and Functionalization of Alkanes, Wiley, New York, 1989, p. 243.
[7] J.F. Keggin, Nature 131 (1933) 908.
[8] J.M. Maestre, C. Bo, J.-M. Poblet, N. Casañ-Pastor, P. Gomez-Romero, Inorg. Chem. 37 (1998) 3444.
[9] I.V. Kozhevnikov, Chem. Rev. 98 (1998) 171.
[10] N. Mizuno, M. Misono, J. Mol. Catal. 86 (1994) 319.
[11] J. Melsheimer, S.S. Mahmoud, G. Mestl, R. Schlögl, Catal. Lett. 60 (1999) 103.
[12] I.V. Kozhevnikov, Catal. Rev.-Sci. Eng. 37 (1995) 311.
[13] O. Watzenberger, G. Emig, D.T. Lynch, J. Catal. 124 (1990) 247.
[14] Y. Seki, J.S. Min, M. Misono, N. Mizuno, J. Phys. Chem. B 104 (2000) 5940.
[15] K. Nomiya, K. Hashino, Y. Nemoto, M. Watanabe, J. Mol. Catal. A 176 (2001) 79.
[16] K. Nomiya, H. Yanagibayashi, C. Nozaki, K. Kondoh, E. Hiramatsu, Y. Shimizu, J. Mol. Catal. A 114 (1996) 181.
[17] N.A. Alekar, V. Indira, S.B. Halligudi, D. Srinivas, J. Mol. Catal. A 164 (2000) 181.
[18] J. Zhang, Y. Tang, G. Li, C. Hu, Appl. Catal. A 278 (2005) 251.
[19] K. Nomiya, S. Matsuoka, T. Hasegawa, Y. Nemoto, J. Mol. Catal. A 156 (2000) 143.
[20] K. Nomiya, K. Yagishita, Y. Nemoto, T. Kamataki, J. Mol. Catal. A 126 (1997) 43.
[21] I.K. Song, M.A. Barteau, J. Mol. Catal. A 212 (2004) 229.
[22] M.T. Pope, T.F. Scully, Inorg. Chem. 14 (1975) 953.
[23] L. Pettersson, I. Andersson, A. Selling, J.H. Grate, Inorg. Chem. 33 (1994) 982.
[24] A. Selling, I. Andersson, J.H. Grate, L. Pettersson, Eur. J. Inorg. Chem. (2000) 1509.
[25] A.M. Khenkin, A. Rosenberger, R. Neumann, J. Catal. 182 (1999) 82.
[26] R.S. Weber, J. Phys. Chem. 98 (1994) 2999.
[27] J.M. Maestre, X. López, C. Bo, J.M. Poblet, N. Casañ-Pastor, J. Am. Chem. Soc. 123 (2001) 3749.
[28] X. López, J.M. Maestre, J.M. Poblet, C. Bo, J. Am. Chem. Soc. 123 (2001) 9571.
[29] M.-M. Rohmer, M. Bénard, J.-P. Blaudeau, J.M. Maestre, J.M. Poblet, Coord. Chem. Rev. 178–180 (1998) 1019.
[30] J.M. Maestre, X. López, C. Bo, J.M. Poblet, Inorg. Chem. 41 (2002) 1883.
[31] A.J. Bridgeman, Chem. Phys. 287 (2003) 55.
[32] N.C. Handy, A.J. Cohen, Mol. Phys. 99 (2001) 403.
[33] W.-M. Hoe, A.J. Cohen, N.C. Handy, Chem. Phys. Lett. 341 (2001) 319.
[34] C. Lee, W. Yang, R.G. Parr, Phys. Rev. B 37 (1988) 785.
[35] A.D. Becke, J. Phys. Chem. 98 (1993) 5648.

[36] J. Baker, P. Pulay, J. Comput. Chem. 24 (2003) 1184.
[37] J.C. Slater, Quantum Theory of Molecules and Solids, vol. 4, The Self-Consistent Field for Molecules and Solids, McGraw-Hill, New York, 1974.
[38] A.D. Becke, Phys. Rev. A 38 (1988) 3098.
[39] S.H. Vosko, L. Wilk, M. Nusair, Can. J. Phys. 58 (1980) 1200.
[40] V.A. Guner, K.S. Khuong, K.N. Houk, A. Chuma, P. Pulay, J. Phys. Chem. A 108 (2004) 2959.
[41] X. Xu, W.A. Goddard, J. Phys. Chem. A 108 (2004) 8495.
[42] E.R. Johnson, R.A. Wolkow, G.A. DiLabio, Chem. Phys. Lett. 394 (2004) 334.
[43] J. Baker, P. Pulay, J. Chem. Phys. 117 (2002) 1441.
[44] T. Strassner, M.A. Taige, J. Chem. Theory Comput. 1 (2005) 848.
[45] H.E. Daniel, K.N. Houk, J. Phys. Chem. A 109 (2005) 9542.
[46] J.D. Larkin, C.W. Bock, H.F. Schaefer, J. Phys. Chem. A 109 (2005) 10100.
[47] R. Cammi, B. Mennucci, J. Tomasi, J. Phys. Chem. A 104 (2000) 5631, and references related.
[48] Gaussian 03, Revision B.05, M.J. Frisch, G.W. Trucks, H.B. Schlegel, G.E. Scuseria, M.A. Robb, J.R. Cheeseman, J.A. Montgomery Jr., T. Vreven, K.N. Kudin, J.C. Burant, J.M. Millam, S.S. Iyengar, J. Tomasi, V. Barone, B. Mennucci, M. Cossi, G. Scalmani, N. Rega, G.A. Petersson, H. Nakatsuji, M. Hada, M. Ehara, K. Toyota, R. Fukuda, J. Hasegawa, M. Ishida, T. Nakajima, Y. Honda, O. Kitao, H. Nakai, M. Klene, X. Li, J.E. Knox, H.P. Hratchian, J.B. Cross, V. Bakken, C. Adamo, J. Jaramillo, R. Gomperts, R.E. Stratmann, O. Yazyev, A.J. Austin, R. Cammi, C. Pomelli, J.W. Ochterski, P.Y. Ayala, K. Morokuma, G.A. Voth, P. Salvador, J.J. Dannenberg, V.G. Zakrzewski, S. Dapprich, A.D. Daniels, M.C. Strain, O. Farkas, D.K. Malick, A.D. Rabuck, K. Raghavachari, J.B. Foresman, J.V. Ortiz, Q. Cui, A.G. Baboul, S. Clifford, J. Cioslowski, B.B. Stefanov, G. Liu, A. Liashenko, P. Piskorz, I. Komaromi, R.L. Martin, D.J. Fox, T. Keith, M.A. Al-Laham, C.Y. Peng, A. Nanayakkara, M. Challacombe, P.M.W. Gill, B. Johnson, W. Chen, M.W. Wong, C. Gonzalez, J.A. Pople, Gaussian, Inc., Wallingford, CT, 2004.
[49] P.J. Hay, W.R. Wadt, J. Chem. Phys. 82 (1985) 270, 299.
[50] C.E. Check, T.O. Faust, J.M. Bailey, B.J. Wright, T.M. Gilbert, L.S. Sunderlin, J. Phys. Chem. A 105 (2001) 8111.
[51] R. Strandberg, Acta Chem. Scand. A 29 (1975) 359.
[52] C. Rocchiccioli-Deltcheff, M. Fournier, R. Franck, R. Thouvenot, Inorg. Chem. 22 (1983) 207.
[53] X. López, C. Bo, J.M. Poblet, J. Am. Chem. Soc. 124 (2002) 12574.
[54] R.D. Gall, M. Faraj, C.L. Hill, Inorg. Chem. 33 (1994) 5015.
[55] M. Tani, T. Sakamoto, S. Mita, S. Sakaguchi, Y. Ishii, Angew. Chem. Int. Ed. 44 (2005) 2586.
[56] S. Shinachi, H. Yahiro, K. Yamaguchi, N. Mizuno, Chem. Eur. J. 10 (2004) 6489.